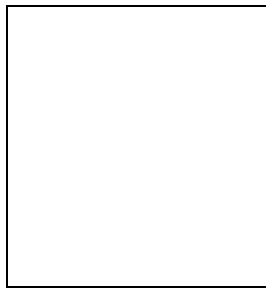


# ON THE NEUTRINO FLUX FROM GAMMA RAY BURSTS: AN OVERVIEW

DAFNE GUETTA

*Osservatorio astrofisico di Arcetri, Largo E. Fermi 5,  
50100 Firenze, Italy*



Observations imply that gamma-ray bursts (GRBs) are produced by the dissipation of the kinetic energy of a highly relativistic fireball. Photo-meson interactions of protons with  $\gamma$ -rays within the fireball dissipation region are expected to convert a significant fraction of the fireball energy into high energy neutrinos. In this talk we summarize the results of an analysis of the internal shock model of GRBs, where production of synchrotron photons and photo-meson neutrinos with energies  $\sim 10^{14}$  eV are self-consistently calculated. These neutrinos will be coincident with the GRB. We show that the fraction of fireball energy converted into high energy neutrinos is not sensitive to uncertainties in the fireball model parameters, such as the expansion Lorentz factor and characteristic variability time. Other processes of neutrinos emission from GRBs are also reviewed. Photomeson interactions within the plasma region shocked by the reverse shock, may produce a burst of  $\sim 10^{18}$  eV neutrinos following the GRB on the time scale of 10 s. Inelastic p-n nuclear collisions result in the production of a burst of  $\sim 10$  GeV neutrinos in coincidence with the GRB. Planned 1 km<sup>3</sup> neutrino telescopes are expected to detect ten 100 TeV neutrino events and several 10<sup>18</sup> eV events, correlated with GRBs, per year. A suitably densely spaced detector may allow the detection of several 10 GeV events per year.

## 1 Introduction

The characteristics of  $\gamma$ -ray bursts (GRBs), bursts of 0.1 MeV–1 MeV photons lasting for a few seconds<sup>1</sup>, suggest that the observed radiation is produced by the dissipation of the kinetic energy of a relativistically expanding wind, a “fireball,” at cosmological distance (see, e.g.,<sup>2</sup> for review). The recent detection of delayed low energy (X-ray to radio) emission (afterglow) from GRB sources (see<sup>3</sup> for review), confirmed both the cosmological origin of the bursts and the standard model predictions for afterglows, that result from the collision of an expanding fireball with its surrounding medium (see<sup>4</sup> for review).

Within the fireball model framework, observed  $\gamma$ -rays are produced by synchrotron emission

of electrons accelerated in the fireball dissipation region. In this region the plasma parameters allow Fermi shock acceleration of protons up to energies  $> 10^{20}$  eV<sup>5,6</sup>; (see<sup>7</sup> for a recent review).

High energy protons may photo-interact with the fireball photons leading to emission of high energy neutrinos<sup>8,9</sup>. Electrons and protons can be accelerated to high energy by internal shocks within the expanding wind or by the reverse shock during the transition of the plasma to self-similarity. In the first case a burst of  $\sim 100$  TeV neutrinos is expected in coincidence with the GRB, and if protons are accelerated in the reverse shock a burst of  $\sim 10^{18}$  eV neutrinos is expected to follow the GRB on a time scale of 10 s. Lower energy neutrinos may be produced by inelastic nuclear collisions<sup>10,11</sup>.

In this review new results found in Guetta, Spada & Waxman 2001 (GSW01)<sup>12</sup> on the  $\nu$  flux expected in the internal shock model scenario are presented and recent work on the high energy neutrino production by GRB fireballs is summarized. Implications for planned  $\sim 1\text{km}^3$  neutrino telescopes (the ICECUBE extension of AMANDA, ANTARES, NESTOR; see<sup>13</sup> for review) are discussed. High energy neutrino production in internal shocks is discussed in § 2, other mechanisms for neutrino production in GRBs are summarized in § 3 and the implications for the planned neutrino telescopes are presented in § 4.

## 2 Internal shocks neutrinos

High energy neutrinos are produced by the decay of charged pions,  $\pi^+ \rightarrow \mu^+ + \nu_\mu \rightarrow e^+ + \nu_e + \bar{\nu}_\mu + \nu_\mu$ , created in interactions between the fireball photons and accelerated protons<sup>8,14</sup>. The characteristic energy of these neutrinos is determined by the relation between the observed photon energy,  $E_\gamma$ , and the accelerated proton's energy,  $E_p$ , at the photo-meson threshold of the  $\Delta$ -resonance. In the observer frame,

$$E_\gamma E_p = 0.2 \text{ GeV}^2 \Gamma^2. \quad (1)$$

For typical observed  $\gamma$ -ray energy of 1 MeV and Lorentz factors of the expanding fireball  $\Gamma \sim 300$ , proton energies  $E_p \approx 2 \times 10^7$  GeV are required to produce neutrinos from pion decay. Typically the neutrinos receive 5% of proton energy leading to  $\nu$  of  $\sim 10^{15}$  eV.

The predicted flux of  $\gtrsim 10^{14}$  eV neutrinos produced in internal shocks is determined by the fraction  $f_\pi$  of fireball proton energy lost to pion production. This fraction is given by  $f_\pi = \min(1, \Delta t/t_\pi)$  where  $\Delta t$  is the comoving shell expansion time and  $t_\pi$  is the proton photo-pion energy loss time. The value of this fraction has been estimated to be<sup>8,14</sup>

$$f_\pi(E_p) \approx 0.2 \min(1, E_p/E_p^b) \frac{L_{\gamma,52}}{\Gamma_{2.5}^4 \Delta t_{-2} E_{\gamma,\text{MeV}}^b}. \quad (2)$$

The  $\gamma$ -ray luminosity  $L_\gamma$ , the photon spectral break energy  $E_\gamma^b$  (where luminosity per logarithmic photon energy interval peaks), the observed variability time  $\Delta t$  and the wind Lorenz factor  $\Gamma$  are normalized in Eq. 2 to their typical values inferred from observations:  $L_\gamma = 10^{52}$  erg/s,  $E_\gamma^b = 1E_{\gamma,\text{MeV}}^b$  MeV,  $\Delta t = 10^{-2}$  s, and  $\Gamma = 10^{2.5}$ . The proton break energy,  $E_p^b$ , is the threshold proton energy for interaction with photons of observed energy  $E_\gamma^b$ ,  $E_p^b = (2/E_{\gamma,\text{MeV}}^b) \Gamma_{2.5}^2 \times 10^7$  GeV. For a typical burst,  $E \approx 10^{53}$  erg at redshift  $z \sim 1$ , Eq. 2 implies a neutrino fluence

$$E_\nu^2 \Phi_\nu \approx 10^{-3} \left( \frac{E_\nu}{E_\nu^b} \right)^\alpha \frac{\text{GeV}}{\text{cm}^2}, \quad (3)$$

where the neutrino break energy is given by  $E_\nu^b \approx 10^{15} \Gamma_{2.5}^2 / E_{\gamma,\text{MeV}}^b$  eV, whereas  $\alpha = 0$  for  $E_\nu > E_\nu^b$  and  $\alpha = 1$  for  $E_\nu < E_\nu^b$ .

The value of  $f_\pi$ , Eq. 2, is strongly dependent on  $\Gamma$ . It has recently been pointed out by Halzen and Hooper<sup>15</sup> that if the Lorentz factor  $\Gamma$  varies significantly between bursts, the

resulting neutrino flux will be dominated by a few neutrino bright bursts, and may significantly exceed the flux given by Eq. 3, derived for typical burst parameters. This may strongly enhance the detectability of GRB neutrinos by planned neutrino telescopes<sup>13</sup>.

In this section we present the most important results of the work GSW01<sup>12</sup> whose main goal has been to determine the allowed range of variation in the fraction of fireball energy converted to high energy neutrinos, under the assumption that GRBs are produced by internal dissipative shocks in an ultra-relativistic wind.

## 2.1 Model dynamics and neutrino production

In the fireball model of GRB<sup>2</sup> a compact source, of linear scale  $R_0 \sim 10^6$  cm, produces a wind characterized by an average luminosity  $L_w \sim 10^{52} \text{ erg s}^{-1}$ – $10^{53} \text{ erg s}^{-1}$  and mass loss rate  $\dot{M} = L_w/\eta c^2$ . Variability of the source on time scale  $\Delta t$ , resulting in fluctuations in the wind bulk Lorentz factor  $\Gamma$  on a similar time scale, leads to internal shocks that can reconvert a substantial part of the kinetic energy to internal energy. It is assumed that this energy is then radiated as  $\gamma$ -rays by synchrotron (and inverse-Compton) emission of shock-accelerated electrons.

In GSW01 we have used an approximate model for the unsteady wind following Spada, Panaiteescu & Mészáros 2000<sup>16</sup>, and Guetta, Spada & Waxman 2000 (GSW00)<sup>17</sup>. The wind flow is approximated as a set of discrete shells. Each shell is characterized by four parameters: the ejection time  $t_j$ , where the subscript  $j$  denotes the  $j$ -th shell, the Lorentz factor  $\Gamma_j$ , the mass  $M_j$ , and the width  $\Delta_j$ . Since the wind duration,  $t_w \sim 10$  s, is much larger than the dynamical time of the source,  $t_d \sim R_0/c$ , variability of the wind on a wide range of time scales,  $t_d < t_v < t_w$ , is possible. For simplicity, we considered a case where the wind variability is characterized by a single time scale  $t_v$ , in addition to the dynamical time scale of the source  $t_d$  and to the wind duration  $t_w$ . Thus, we considered shells of initial thickness  $\Delta_j = ct_d = R_0$ , ejected from the source at an average rate  $t_v^{-1}$ . In GSW00 we examined the dependence of the observed  $\gamma$ -ray flux and spectrum on wind model parameters, taking into account both synchrotron and inverse-Compton emission, and the effect of  $e^\pm$  pair production. We have shown that in order to obtain  $\gamma$ -ray fluxes and spectra consistent with observations, large variance is required in the wind Lorentz factor distribution. We therefore restricted our study to the bimodal case, where Lorentz factors are drawn from a bimodal distribution,  $\Gamma_j = \Gamma_m$  or  $\Gamma_j = \Gamma_M \approx \eta_* \gg \Gamma_m$ , with equal probability. The time intervals  $t_{j+1} - t_j$  were drawn randomly from a uniform distribution with an average value of  $t_v$ . In GSW00 we considered two qualitatively different scenarios for shell masses distribution, shells of either equal mass or equal energy, and concluded that observations favor shells of equal mass. We therefore restricted our analysis to the equal shell mass case.

Once the shell parameters had been determined, we calculated the radii where collisions occur and determined the photon and neutrino emission from each collision. In each collision a forward and a reverse shock are formed, propagating into forward and backward shells respectively. We assumed that a fraction  $\epsilon_e$  of the protons shock thermal energy is converted to electrons and a fraction  $\epsilon_B$  to magnetic field. We adopted these fractions to be close to equipartition,  $\epsilon_e = 0.45$  and  $\epsilon_B \gtrsim 0.01$ . We further assumed that both electrons and protons are accelerated by the shocks to a power-law distribution,  $dn_\alpha/d\gamma_\alpha \propto \gamma_\alpha^{-p}$ , with  $p \approx 2$  for particle Lorentz factors  $\gamma_{\alpha,\min} < \gamma_\alpha < \gamma_{\alpha,\max}$ . The maximum Lorenz factor is determined by equating the acceleration time, estimated as the Larmor radius divided by  $c$ , to the minimum between the dynamical and synchrotron cooling time.

The calculation of the emitted  $\nu$  spectrum and flux was carried out according to the method described in GSW01, following Waxman & Bahcall 1997<sup>8</sup>. Photo-meson production of low energy protons, well below  $E_p^b$ , requires interaction with high energy photons, well above  $E_\gamma^b$ . Such photons may be depleted by pair production. For each collision we found the photon

energy  $E_\gamma^\pm$ , for which the pair production optical thickness,  $\tau_{\gamma\gamma}$ , is unity. A large fraction of photons of energy exceeding  $\max(E_\gamma^\pm, m_e c^2)$  (measured in the shell frame) will be converted to pairs, and hence will not be available for photo-meson interaction, leading to a suppression of the neutrino flux at low energies. In order to take this effect into account, we used  $f_\pi = \min[1, (\Delta t/t_\pi) \min(1, \tau_{\gamma\gamma}^{-1})]$  for protons interacting with photons which are strongly suppressed by pair production.

Neutrino production is suppressed at high energy, where neutrinos are produced by the decay of muons and pions whose lifetime  $\tau$  exceeds the characteristic time for energy loss due to synchrotron emission<sup>8,14,18</sup>. We therefore defined an effective  $f_\pi$ ,  $f_{\pi,\text{eff.}}$ , as  $4f_\pi$  times the fraction of pions' energy converted to muon neutrinos.

In each collision a fraction of the kinetic energy of the colliding shell is converted to a flux of photons and neutrinos. The energy that is not lost to photons and neutrinos is converted back to kinetic energy by adiabatic expansion of the shell.

## 2.2 Main results and conclusions

The main results of GWS01 are presented in Figures 1 and 2. Figure 1 presents the contour plot for the effective  $f_\pi$ ,  $f_{\pi,\text{eff.}}$  taking  $\epsilon_B = 0.01$ . The values shown are averaged over all internal collisions, weighted by the energy converted to high energy protons in each collision. Values of  $f_\pi$  are shown for several neutrino energy ranges, using the approximation  $E_\nu = 0.05E_p$ . The region in  $\Gamma_m-t_\nu$  plane where  $E_\nu^b > 0.1$  MeV is bound in Figures 1 by the dashed line. The dash-dotted line outlines the region in which the fraction of wind energy converted to radiation exceeds 2% (higher fraction is obtained for larger  $\Gamma_m$  values). Figure 2 shows the contour plots of  $f_\pi$ , neglecting the effects on neutrino production of synchrotron losses and pair-production.  $f_\pi$  approaches unity at low values of  $\Gamma_m$  for low proton (neutrino) energies, and at intermediate values of  $\Gamma_m$  for high proton (neutrino) energies. The energy loss of pions and muons due to synchrotron emission reduces the fraction of pion energy converted to neutrinos, and hence suppresses the effective value of  $f_\pi$ , to the range of values shown in Figure 1. The suppression seen in Figure 2 of  $f_\pi$  at low  $\Gamma_m$  for high energy protons is due to the fact that for low values of  $\Gamma_m$  most collisions occur at small radii, where synchrotron losses of high energy protons prevent acceleration of protons to ultra-high energy<sup>5</sup>. Ultra-high energy protons are produced in this case only by secondary collisions at large radii, where the photon energy density is already low, resulting in smaller values of  $f_\pi$ .

As we can see from Figure 1, for wind parameters consistent with observed GRB characteristics, the effective value of  $f_\pi$  at high neutrino energies,  $E_\nu > E_\nu^b$ , is restricted to values in the range of  $\approx 10\%$  to  $\approx 30\%$ . The weak dependence of  $f_{\pi,\text{eff.}}$  on wind the model parameters, in contrast with the strong dependence implied by Eq. 2, is due to two reasons. First, for low values of  $\Gamma$  and  $\Delta t$ , where large values of  $f_\pi$  are implied by Eq. 2, only a small fraction of the pions' energy is converted to neutrinos at high proton energy due to pion and muon synchrotron losses (compare figures 1 and 2). Second, the observational constraints imposed by  $\gamma$ -ray observations imply that the wind model parameters ( $\Gamma$ ,  $L$ ,  $\Delta t$ ) are correlated. From Figure 1 we note, also, that the value of  $f_{\pi,\text{eff.}}$  does not significantly exceed 20% also in wind model parameter regions which are outside the parameter region implied by observations. Our results imply that GRB neutrino flux of individual bursts should correlate mainly with the bursts'  $\gamma$ -ray flux.

## 3 Neutrinos from other processes in GRBs

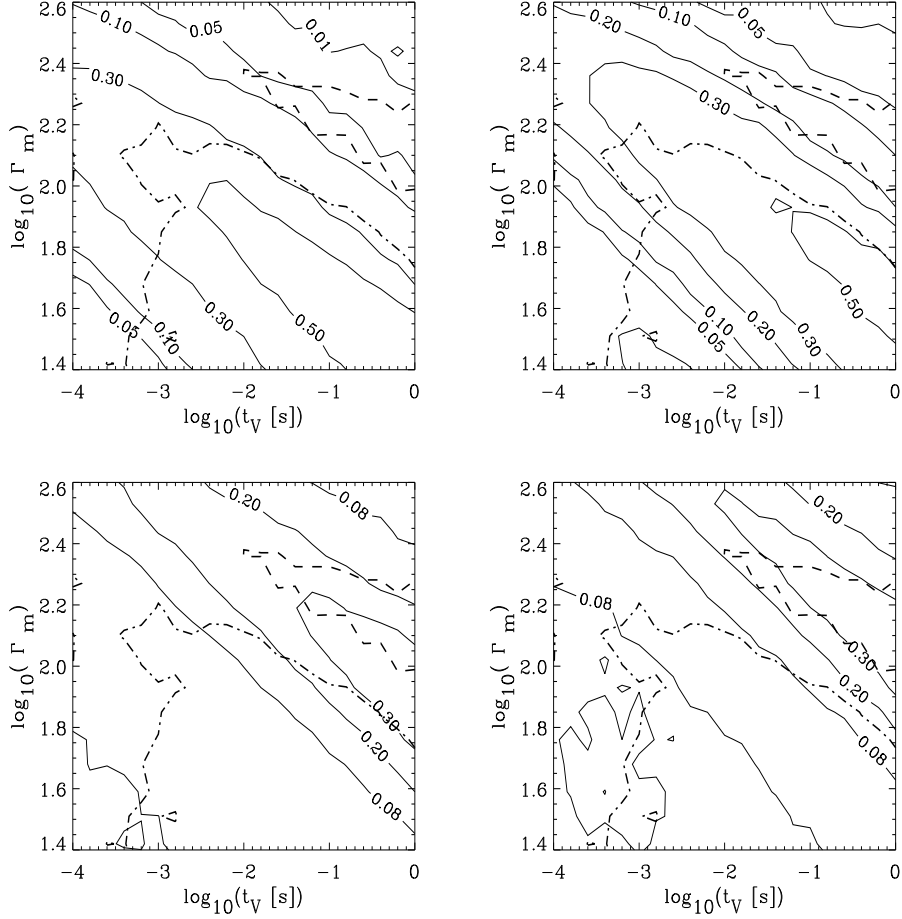


Figure 1: Contour plots of  $f_{\pi, \text{eff.}}$ , the effective value of  $f_\pi$  (defined as  $4f_\pi$  times the fraction of pions' energy converted to muon neutrinos), as function of wind variability time  $t_v$  and minimum Lorentz factor  $\Gamma_m$ , for wind luminosity  $L_w = 10^{53} \text{ erg/s}$  and  $\epsilon_B = 0.01$ . The four panels correspond to four observed neutrino energy bins, clockwise from top left:  $10^{14} \text{ eV} < E_\nu < 10^{15} \text{ eV}$ ,  $10^{15} \text{ eV} < E_\nu < 10^{16} \text{ eV}$ ,  $10^{17} \text{ eV} < E_\nu < 10^{18} \text{ eV}$ ,  $10^{18} \text{ eV} < E_\nu < 10^{19} \text{ eV}$ . We have used the approximate relation  $E_\nu = 0.05 E_p$  between neutrino and proton energy, and assumed a source redshift  $z = 1.5$ . The region in the  $\Gamma_m$ - $t_v$  plane where  $E_\gamma^b > 0.1 \text{ MeV}$  is bound by the dashed lines. The dash-dotted lines outline the region in which the fraction of wind energy converted to radiation exceeds 2% (a higher fraction is obtained at larger  $\Gamma_m$  values).

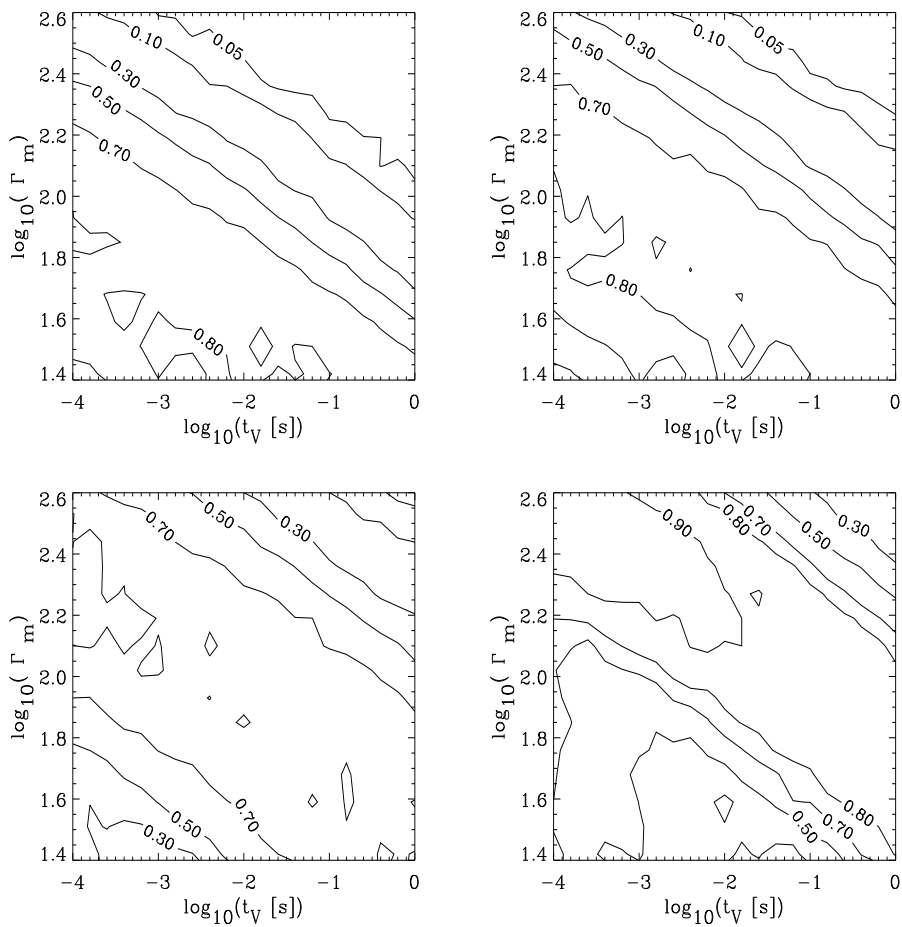


Figure 2: Contour plots of  $f_\pi$ , obtained when the effects on neutrino production of synchrotron losses and pair-production are neglected, for the case shown in Figure 1.

### 3.1 Neutrinos from the reverse shock

Much higher energy,  $\gtrsim 10^{18}$  eV, neutrinos may be produced at a later stage, at the onset of the fireball interaction with its surrounding medium. During the transition to self-similar expansion, which takes place on time scale  $\sim t_w$ , protons and electrons are accelerated in the reverse shocks. The combination of low energy photons, 10 eV-1 keV, and high energy protons produces neutrinos of ultra-high energy  $10^{17} - 10^{19}$  eV via photo-meson interactions, as indicated by Eq. 1<sup>9</sup>. However, the fraction of energy converted to pions depends upon parameters of the surrounding medium. If the density of the surrounding gas is that typical of the interstellar medium  $n_0 \sim 1\text{cm}^{-3}$ , the photon emission peaks in the X-ray band,  $E_{\gamma,\text{keV}}^b$  and the luminosity is  $L_X \approx 10^{50}\text{erg/s}$ . Using these parameters in Eq. 1, replacing  $\Delta t$  with  $t_w$  and considering that the self-similar Lorentz factor of the expanding plasma under these conditions is  $\Gamma_{\text{BM}} \sim 250$ , we find  $f_\pi = 0.01$ . Thus the expected neutrino fluence for a typical burst,  $E \approx 10^{53}$  erg at  $z \sim 1$ , is<sup>9</sup>

$$E_\nu^2 \Phi_\nu \approx 10^{-4.5} \left( \frac{E_\nu}{E_\nu^b} \right)^\alpha \frac{\text{GeV}}{\text{cm}^2}, \quad (4)$$

where  $E_\nu^b \sim 10^{17}$  eV,  $\alpha = 1/2$  for  $E_\nu < E_\nu^b$  and  $\alpha = 1$  for  $E_\nu > E_\nu^b$ . If the fireball expands into a pre-existing wind, the transition to self-similar behaviour takes place at a radius where the wind density is  $n \approx 10^4\text{cm}^{-3}$ . Since  $\Gamma_{\text{BM}}$  decreases with increasing density, according to Eq. 1 protons of energy  $E_p > 10^{18}$  eV lose all their energy to pion production in the wind case, and a typical GRB at  $z \sim 1$  is expected to produce a neutrino fluence<sup>9</sup>

$$E_\nu^2 \Phi_\nu \approx 10^{-2.5} \left( \frac{E_\nu}{E_\nu^b} \right)^\alpha \frac{\text{GeV}}{\text{cm}^2}, \quad (5)$$

where again  $E_\nu^b \sim 10^{17}$  eV,  $\alpha = 0$  for  $E_\nu < E_\nu^b$  and  $\alpha = 1$  for  $E_\nu > E_\nu^b$ .

### 3.2 Inelastic p-n collisions

We briefly discuss how lower energy neutrinos may be produced by inelastic nuclear collisions, a detailed analysis of these processes is given in<sup>11,10</sup>. According to most progenitor scenarios neutrons can contribute to the barionic component of the fireball as much as protons. During the acceleration phase of the fireball protons and neutrons are coupled by nuclear scattering. As the fireball expands neutrons and protons may decouple and relativistic relative velocities may arise between them, leading to pion production through unelastic collisions. Since the decoupling happens when the wind Lorentz factor is  $\sim 400$ , neutrons decouple from the accelerating plasma prior to saturation,  $\Gamma = \eta$ , only if  $\eta > 400$ . Charged pions may decay in  $\sim 10$  GeV neutrinos. A typical burst,  $E = 10^{53}$  erg at  $z \sim 1$ , with a significant neutron to proton ratio and  $\eta > 400$  will produce a fluence of  $\sim 10^{-4}\text{cm}^{-2}$  of  $\sim 10$  GeV neutrinos.

## 4 Implications

The high energy neutrinos predicted in the dissipative wind model of GRBs may be observed by detecting the Cerenkov light emitted by high energy muons produced by neutrino interactions below a detector on the surface of the Earth (see<sup>19</sup> for a recent review).

For the internal shocks neutrinos with energies  $10^{14} - 10^{15}$  eV, the fluence found in Eq. 3 implies a detection probability of  $\sim 0.03$  per burst in a km-cube telescope, corresponding to tens of events per years correlated in time and direction with GRBs, given the observed GRB rate of  $\approx 10^3\text{yr}^{-1}$ . The predicted fluence of neutrinos of  $10^{17}$  eV produced during the transition of the fireball to self-similarity depends strongly upon the conditions of the surrounding gas. In the case of a fireball expanding in a typical interstellar medium Eq. 4 implies a detection probability

of  $\sim 10^{-4.5}$  per burst in a km-cube telescope. This probability is higher,  $\sim 10^{-2.5}$ , in the case of fireball expansion into a pre-existing massive star wind. In this case a  $\text{km}^3$  telescope should detect several muon induced neutrinos per year.

Inelastic p-n collisions may produce neutrinos of  $\sim 10$  GeV with a fluence of  $\sim 10^{-4} \text{ cm}^{-2}$  per burst, due to the decoupling of neutrons and protons during the acceleration phase. This process is possible only if large neutron to proton ratio and high,  $> 400$ , Lorentz factor are assumed. Ten events per year are expected in a  $\text{km}^3$  detector. Such events may be detectable in a suitably densely spaced detector.

Detection of high energy neutrinos will test the shock acceleration mechanism and the suggestion that GRBs are the sources of ultra-high energy protons, since  $\geq 10^{14}$  eV ( $\geq 10^{18}$  eV) neutrino production requires protons of energy  $\geq 10^{16}$  eV ( $\geq 10^{19}$  eV). Detection of  $\sim 10$  GeV neutrinos will constrain the fireball neutron fraction, and hence the GRB progenitor.

## Acknowledgments

I thank Eli Waxman for his fundamental help in preparing this review and the original work contained in it.

## References

1. Fishman, G. J. & Meegan, C. A., ARA&A **33**, 415, (1995).
2. Piran, T., Phys. Rep. **314**, 575, (1999).
3. Kulkarni, S. R. *et al.*, To appear in Proc. of the 5th Huntsville Gamma-Ray Burst Symposium (astro-ph/0002168).
4. Mészáros, P., A&AS **138**, 533, (1999).
5. Waxman, E., Phys. Rev. Lett. **75**, 386, (1995).
6. Vietri, M., Ap. J. **453**, 883, (1995).
7. Waxman, E., Nucl. Phys. B (Proc. Suppl.) **87**, 345, (2000).
8. Waxman, E., & Bahcall, J. N., Phys. Rev. Lett. **78**, 2292, (1997).
9. Waxman, E., & Bahcall J. N., Ap. J. **541**, 707, (2000).
10. Bahcall, J. N., & Mészáros, P., Phys. Rev. Lett. **85**, (2000).
11. Mészáros, P., & Rees, M., Ap. J. **541**, L5, (2000).
12. Guetta, D., Spada, M., & Waxman, E., astro-ph/0102487, submitted to Ap. J., (GSW01)
13. Alvarez-Muniz, J., Halzen, F., & Hooper, D. W., Phys. Rev. **D62**, 093015, (2000).
14. Waxman, E., & Bahcall, J. N., Phys. Rev. **D 59**, 023002, (1999).
15. Halzen, F. & Hooper, D. W., ApJ, 527, L93, (1999).
16. Spada, M., Panaitescu, A., & Mészáros, P., Apj, **537**, 824, (2000).
17. Guetta, Spada & Waxman, astro-ph/0011170, to appear in Ap. J. (GSW00).
18. Rachen P. & Mészárós P., Phys. Rev. **D 58**, 123005, (1998).
19. Gaisser, T. K., Halzen, F., & Stanev, T., Phys. Rep. **258**, 173, (1995).